https://doi.org/10.31925/farmacia.2025.6.24 **ORIGINAL ARTICLE**

EFFECTS OF PAEONIFLORIN EXTRACT-MEDIATED miRNA-140 TARGETING OF WNT/β-CATENIN SIGNALLING PATHWAY ON PROLIFERATION AND APOPTOSIS OF CHONDROCYTES IN OSTEOARTHRITIS

CHANGSHEN BAO, JIAN LUO, YONGJUN MENG, ZHICHAO GAO *

Department of Orthopaedics, First People's Hospital of Linping District, Hangzhou 311100, Zhejiang, China

**corresponding author: gaozhichaozj@163.com*

Manuscript received: October 2025

Abstract

The aim of this study was to evaluate the effects of paeoniflorin extract (Pae) on chondrocyte proliferation and apoptosis in osteoarthritis, with emphasis on miR-140 regulation and modulation of the Wnt/β-catenin signalling pathway. The work comprised two components. First, paeoniflorin extract was characterised, and its pharmacokinetics were assessed following oral administration and intestinal perfusion. Second, its anti-inflammatory efficacy was examined in an IL-1β-stimulated human chondrocyte model (C28/I2). *In vitro* within-day precision ranged from 2.16% to 4.27%, inter-day precision from 1.85% to 5.08%, recovery was 72.88% - 77.41%, and relative standard deviation values were all < 15%. After gavage, effective intestinal permeability coefficients were 0.26 - 0.34, with peak plasma concentrations at 3 - 4 hours; absorption and elimination half-lives ranged from 0.667 - 1.124 h and 1.250 - 1.881 h, respectively. *In vitro*, IL-1β reduced cell proliferation, increased apoptosis, downregulated miR-140, DVL2, Cyclin D1 and β-catenin, and upregulated GSK-3β ($p < 0.05$). Treatment with low, medium and high concentrations of Pae reversed these effects in a dose-dependent manner ($p < 0.05$). Overall, paeoniflorin extract upregulated miR-140 and modulated Wnt/β-catenin signalling, thereby attenuating IL-1β-induced chondrocyte dysfunction.

Rezumat

Scopul acestui studiu a fost de a evalua efectele extractului de paeoniflorină (Pae) asupra proliferării și apoptozei condrocitelor în osteoartrită, cu accent pe reglarea miR-140 și modularea căii de semnalizare Wnt/β-catenină. Lucrarea a abordat două aspecte: caracterizarea extractului prin evaluarea farmacocinetica a acestuia după administrare orală și perfuzie intestinală și investigarea efectului antiinflamator într-un model *in vitro* de condrocite umane C28/I2 stimulate cu IL-1β. După administrarea orală, coeficienții de permeabilitate intestinală au avut valori de 0,26 - 0,34, cu concentrație plasmatică maximă la 3 - 4 ore. Timpii de înjumătățire pentru absorbție și eliminare au fost 0,667 - 1,124 h și 1,250 - 1,881 h. *In vitro*, IL-1β a redus proliferarea celulară, a crescut apoptoza, a scăzut expresia miR-140, DVL2, Cyclin D1 și β-catenină și a crescut expresia GSK-3β ($p < 0,05$). Tratamentul cu Pae în concentrații mici, medii și mari a inversat aceste efecte într-o manieră dependentă de doză ($p < 0,05$). *Per* ansamblu, extractul de paeoniflorină a crescut nivelul miR-140 și a modulat calea Wnt/β-catenină, ameliorând disfuncția condrocitelor indusă de IL-1β.

Keywords: paeoniflorin extract, pharmacokinetic characteristics, osteoarthritis, interleukin-1β, miR-140, Wnt/β-catenin signalling pathway

Introduction

Osteoarthritis is a common degenerative disease characterised by the destruction of joint matrix and a reduction in joint cells, primarily affecting the elderly population, with a higher incidence in women than in men [1-3]. The pathogenesis of osteoarthritis is associated with various factors, although it has not been fully elucidated. Abnormalities in chondrocytes, specifically in cell proliferation and cell apoptosis, exert a crucial effect in the occurrence and progression of this disease [4]. Therefore, inhibiting chondrocyte apoptosis is one of the therapeutic approaches for treating osteoarthritis.

Traditional Chinese medicine (TCM) approaches, including syndrome differentiation, pattern identification and the adjustment of herbal prescriptions based on individual conditions, have shown positive effects in the clinical treatment of osteoarthritis. TCM can slow down the degeneration of chondrocytes, promote cell proliferation and inhibit apoptosis through mechanisms such as clearing oxygen free radicals, reducing oxidative stress reactions, regulating microcirculation and suppressing the release of inflammatory factors [5]. *Paeonia lactiflora* is a commonly used Chinese herbal medicine belonging to the *Paeoniaceae* family. It possesses pharmacological properties such as heat-clearing, blood-cooling, blood-supplementing, Yin-restraining and pain-relieving effects. Various parts of the peony plant, including the root, stem, leaves and flowers, contain rich chemically active components such as monoterpene glycosides, triterpenes, flavonoids,

volatile oils and phenolic acids, exhibiting anti-inflammatory, anti-cancer and immune-regulating effects [6, 7]. Monoterpenes and their glycoside compounds are the main active ingredients in peony, including paeoniflorin, paeonol glycosides and oxidised paeoniflorin. Paeoniflorin has been shown to improve depressive symptoms by regulating the expression of clock genes in the hippocampus [8]. Additionally, paeoniflorin can inhibit the proliferation, invasion and migration of colon cancer cells [9] and has immune-modulating functions. *In vitro*, paeoniflorin enhances the release of interleukin-1 from splenic cells and peritoneal macrophages, exerting a concentration- and function-dependent bidirectional immune-modulating effect [10]. Studies have confirmed that paeoniflorin can suppress the elevation of inflammatory factors such as tumour necrosis factor-alpha and interleukin (IL)-6 caused by arthritis, exhibiting anti-inflammatory effects [11, 12]. The therapeutic effect of paeoniflorin in the treatment of rheumatoid arthritis is comparable to methotrexate, with lower adverse reactions. Consequently, it has been approved as a Class II western medicine for the treatment of rheumatoid arthritis [13]. However, with the deepening of research on the pharmacokinetic parameters of paeoniflorin and its distribution in tissues *in vivo*, it has been discovered that its bioavailability is relatively low, and there is significant variability in absorption after oral administration.

The Wnt/β-catenin signalling pathway is involved in regulating various biological processes, including cell proliferation and cell apoptosis. In osteoarthritis, abnormal activation of the Wnt/β-catenin signalling pathway is observed, and inhibiting Wnt can regulate the metabolism of chondrocytes and the fibrosis of synovial fibroblasts, thereby playing a therapeutic role in osteoarthritis [14]. Micro ribonucleic acid (miRNA) can specifically recognize binding sites in the 3' non-coding region of mRNA. After complementary base pairing, it affects its transcription and expression, thus regulating cellular biological processes. MiR-140 is highly specifically expressed in cartilage tissue [15].

Therefore, this work explored whether paeoniflorin affects the cell proliferation and cell apoptosis of chondrocytes in osteoarthritis by regulating the expression of miR-140 and activating the Wnt/β-catenin signalling pathway. It aimed to understand the protective mechanism of Paeoniflorin on chondrocytes in osteoarthritis and provide experimental evidence for the development of novel drugs for osteoarthritis.

Materials and Methods

Preparation of paeoniflorin extract solution

9.61 mg of paeoniflorin (Sigma-Aldrich, USA) was dissolved in 1 mL of dimethyl sulfoxide (DMSO) (Sigma-Aldrich, USA), which was then made up to 2 mL with anhydrous ethanol and thoroughly mixed to obtain a 10 mmol/L for the reference solution. This reference solution would be used for subsequent intestinal perfusion experiments and stability tests. Next, 5.85 mg of ginkgolide B (Sigma-Aldrich, USA) was dissolved in a methanol solution, creating a 5.85 mg/L internal standard solution.

Determination of paeoniflorin extract

Methodological detections. Paeoniflorin was quantitatively detected employing ginkgolide B as the internal standard. A Shimadzu octadecylsilyl column (4.6 × 250 × 2.0 mm) was employed, with a mobile phase consisting of a methanol-water solution (70:30). The flow rate was set at 0.22 mL/min, and the column temperature was maintained at 35°C. A sample injection volume of 10 μL was used. Paeoniflorin and ginkgolide B were detected at a wavelength of 230 and 220 nm, respectively.

Plasma sample pretreatment. Whole blood was collected from clean-grade Sprague-Dawley (SD) rats (Beijing BeYou Biotechnology Co., Ltd., China). After the centrifugation, a precise volume of 100 μL of plasma was carefully transferred into a centrifuge tube. Subsequently, 10 μL of ginkgolide B reference solution was added, followed by thorough vortex mixing. A total of 1000 μL of ethyl acetate extraction solution was then added, and the mixture was vortexed before centrifuging at 12,000 rpm for 5 minutes. The upper organic phase was collected, and under 45°C, a water bath and nitrogen gas were used to evaporate the solvent. Afterward, 50 μL of mobile phase was added to dissolve the residue, and 20 μL of the supernatant was taken for injection.

Precision experiment. Blank plasma was utilised to prepare drug-containing samples at drug concentrations of 10, 100, 500, 1000 and 5000 μg/L, along with ginkgolide B reference samples for quality control. For each concentration, five sample analyses were conducted over five consecutive days. Within a single day, five measurements were taken, and the concentration mean, standard deviation and relative standard deviation were calculated. The resulting relative standard deviation (RSD) values for each concentration daily were defined as within-day precision. After performing five measurements on different days over a 5-day period, the calculated relative standard deviation values were defined as intra-day precision.

Experiment for recovery rate. Drug-containing samples at drug concentrations of 10, 100, 500, 1000 and 5000 μg/L were prepared using blank plasma, along with ginkgolide B reference samples for quality control. The reference solution was placed in an empty centrifuge tube, and after nitrogen gas drying, 100 μL of blank plasma was added. Following plasma pretreatment, high-performance liquid chromatography (HPLC) was employed for detection. Four measurements were taken within a single day. After constructing a standard curve, paeoniflorin concentrations were calculated to determine the intra-day recovery rate.

Stability test. Drug-containing samples were prepared in blank plasma at drug concentrations of 10, 100, 500,

1000 and 5000 μg/L, and ginkgolide B reference samples were used for quality control. After plasma pretreatment, each sample was assigned to three aliquots. One aliquot of the sample was left at room temperature for 1, 3, 6 and 12 hours to assess sample stability under ambient conditions. Another aliquot was subjected to three freeze-thaw cycles by placing it in a -20°C freezer and then thawing it, and the stability of the sample under repeated freeze-thaw cycles was assessed. The third aliquot was stored in a -20°C freezer for 5 days to evaluate sample stability under frozen conditions.

In vivo leverage treatment. The animal experiment was approved by the Ethical Committee of First People's Hospital of Linping District, Hangzhou, China. Before the experiment, 15 SD male rats (3 months age) were subjected to a fasting period of at least 18 hours with free access to water. Subsequently, they received an intramuscular injection of 2.3 mL/kg 50% urethane (Shandong Qilu Xinghua Pharmaceutical Co., Ltd., China) for anaesthesia. Blood was drawn *via* the neck vein immediately after intubation with heparin infusion. Blood samples were collected at the perfusion time point. After opening the abdominal cavity, catheters were inserted and ligated at both ends of the duodenum, jejunum, ileum and colon, with each intestinal segment approximately 10 cm. Sterile gauze soaked in physiological saline was applied and covered at the incision site to keep it moist. Using 37°C warm physiological saline, the intestines were washed at a flow rate of 5 mL/min until clean. Afterward, the solution was changed to Hank's Balanced Salt Solution containing drugs at concentrations of 5, 10 and 20 μg/mL. Perfusion was continued at a flow rate of 0.15 mL/min for 50 minutes to reach equilibrium. Subsequently, perfusate was collected every 30 minutes, and the weight was measured. The lengths of various intestinal segments were measured at the end of the experiment. After precise collection of 400 μL of intestinal perfusate, 100 μL of ginkgolide B internal standard solution was added, mixed and centrifuged at 12,000 rpm for 10 min. The supernatant was then taken for analysis. Drug effective permeability coefficient was determined using the weight method.

Pharmacokinetic experiment. Before the experiment, 15 SD male rats were subjected to an 18-hour fasting period with free access to water. The drug was administered *via* oral gavage using Hank's Balanced Salt Solution containing drug concentrations of 5, 10 and 20 μg/mL. Blood samples (0.5 mL) were collected from the retro-orbital venous plexus at 0.0, 0.5, 1.0, 1.5, 2.0, 2.5, 3.0, 4.0, 5.0, 6.0, 9.0, 12.0 and 24.0 hours. After anticoagulation with heparin, the samples were left to stand at room temperature for 1 hour, then centrifuged at 5000 rpm for 10 minutes, and the plasma was collected for analysis. The pharmacokinetic model was fitted using the 3P97 practical pharmacokinetics software developed by the Pharmacometrics Committee of the Chinese Pharmacological Society, and pharmacokinetic parameters were calculated.

Culture, grouping and detection of chondrocytes of osteoarthritis

Preparation and grouping of chondrocytes of osteoarthritis model. The human normal chondrocyte cell line C28/I2 (Chinese Cell Resource Centre, China) was cultured in Dulbecco's Modified Eagle Medium/ Nutrient Mixture F-12 (DMEM/F-12) medium (Gibco, USA) containing 10% FBS and 1% penicillin-streptomycin. The cells were maintained in a 37°C, 5% CO_2 incubator. When the cell confluence reached approximately 80%, they were passaged after trypsin digestion. For seeding, C28/I2 lines were plated in a 96-well plate at 1×10^4 cells/mL.

Control group: The C28/I2 lines were grouped as Control group (normal culture of C28/I2 cells in regular culture medium);

IL-1β group: C28/I2 cells cultured in medium containing 10 ng/mL IL-1β to induce an osteoarthritis chondrocyte model;

IL-1β+L-Pae group: C28/I2 cells cultured in medium containing 10 ng/mL IL-1β and 5 μg/mL paeoniflorin extract;

IL-1β+M-Pae group: C28/I2 cells cultured in medium containing 10 ng/mL IL-1β and 10 μg/mL paeoniflorin extract;

IL-1β+H-Pae group: C28/I2 cells cultured in medium containing 10 ng/mL IL-1β and 20 μg/mL paeoniflorin extract.

Methylthiazolyldiphenyl-tetrazolium bromide (MTT) for detecting cell proliferation. For the grouped culture of C28/I2 cells, at 12, 24, 48 and 72 hours of culture, cell proliferation was assessed using the MTT cell proliferation assay kit (Sigma-Aldrich, USA) following the kit's instructions. In each well, 20 μL of 5 g/L MTT reagent was added, and the cells were incubated at room temperature for 4 hours. The original culture medium was then discarded, and 150 μL of DMSO was introduced. The plate was shaken to mix thoroughly, and the optical density of each well was measured at 490 nm using a SpectraMax i3x Multimode Plate Reader (Shanghai Meigu Molecular Instrument, China).

Flow cytometry (FCT) for cell apoptosis. After 48 hours of grouped culture of C28/I2 cells, the cells were harvested and digested. The detection of cell apoptosis was performed using the Annexin V-Fluorescein Isothiocyanate/Propidium iodide (Annexin V-FITC/PI) assay kit (Sigma-Aldrich, USA). The collected cells were resuspended in 400 μL of binding buffer, followed by the addition of 10 μL of Annexin V-FITC reagent. The mixture was gently mixed and incubated in the dark at room temperature for 15 minutes. Subsequently, 5 μL of PI reagent was added, mixed gently and incubated in the dark at room temperature for an additional 5 minutes. Afterward, 100 μL of binding buffer was added, and the mixture was gently mixed before being analysed using a

CytoFLEX flow cytometer (FCT, Beckman Coulter, USA).

Real-time fluorescence quantitative PCR (rt-qPCR). Grouped cultivation of C28/I2 cells was conducted, and after 48 hours of cultivation, the cells were digested and collected. Total RNA from the cells was extracted using the Trizol reagent method, and the concentration and purity of RNA were determined. Following the instructions of the cDNA reverse transcription kit (Beijing Baorui Doctor Biotechnology Co., Ltd., China), cDNA was synthesized using the extracted RNA as a template. Using cDNA as a template, the TB Green rt-qPCR detection kit (Beijing Baorui Doctor Biotechnology Co., Ltd., China) was utilised to amplify and detect the expression of the target gene according to its instructions. The primers for miR-140 were as follows: upstream: 5'-GAGTGTCAGTGGTTTTACCCT-3', downstream: 5'-GCAGGGTCCGAGGTATTC-3'; for U6, upstream: 5'-GTCGTATCCAGTGCAGGGTCCG-3', downstream: 5'-TGCGGGTGCTCGCTTCGGCAGC-3'. The PCR amplification conditions were as follows: pre-denaturation at 95°C for 5 min, denaturation at 95°C for 30 s, annealing at 60°C for 30 s, extension at 72°C for 50 s, a total of 32 cycles, and final extension at 72°C for 10 min. Using U6 as the reference gene, the relative expression of miR-140 was detected by the $2^{-\Delta\Delta Ct}$ method.

Western blot

C28/I2 cells were subjected to grouped cultivation, and after 48 hours of cultivation, cells were digested and collected. Total cellular proteins were extracted using the RIPA reagent method, and protein concentration was determined using the Bicinchoninic Acid (BCA) protein quantification kit (Thermo Fisher Scientific, China). Sodium dodecyl sulfate-polyacrylamide gel electrophoresis (SDS-PAGE) was employed to separate the proteins, which were then transferred onto a PVDF membrane. The membrane was blocked with 5% skim milk at 37°C for 1 hour. Diluted primary antibodies for DVL2, GSK-3β, cyclin D1, β-catenin and β-actin were added and incubated overnight at 4°C. The membrane was washed three times with Tris-HCl + Tween (TBST), each time for 10 minutes. Diluted secondary antibodies were added and incubated at room temperature for 1 hour. The membrane was washed again three times with TBST, each time for 10 min. Enhanced Chemiluminescence (ECL) chemiluminescent reagent kit (Thermo Fisher Scientific, China) was adopted for visualisation. β-actin was undertaken as the internal reference gene, and protein bands were photographed and analysed for grayscale values using the WD-9403C gel imaging system (Beijing 61Bio Science & Technology Co., Ltd., China). All protein antibodies were obtained from Abcam, UK.

Statistical analysis

Data were statistically analysed using SPSS 22.0. The data were expressed as mean ± RSD. The t-test was employed for comparisons between two groups, while one-way analysis of variance (ANOVA) was utilised for comparisons among multiple groups. A value of $p < 0.05$ was considered statistically significant.

Results and Discussion

Properties of paeoniflorin extract

Figure 1 illustrates the precision, recovery and stability results of paeoniflorin extract at 10, 100, 500, 1000 and 5000 μg/L. It was observed that within-day precision was greater than 2.1%, the inter-day precision exceeded 1.5%, and the recovery rate was above 72.5% for different concentrations of paeoniflorin extract. Additionally, the RSD values were all below 15% for samples placed at room temperature for different durations, subjected to repeated freeze-thaw cycles, and stored under freezing conditions.

Pharmacokinetic characteristics of paeoniflorin extract

Intestinal absorption of paeoniflorin. Figure 2 depicts the HPLC profiles and the drug effective permeability coefficients of rat intestinal perfusate samples after oral gavage with varying concentrations of paeoniflorin extract. As demonstrated in Figure 2A, the blank intestinal perfusate sample (0 μmol/L) displayed only one characteristic peak. In contrast, the intestinal perfusate samples after oral gavage with 5, 10 and 20 μg/mL concentrations of Paeoniflorin extract exhibited three characteristic peaks. The first peak was identical to the characteristic peak in the blank intestinal perfusate sample, the second peak corresponded to paeoniflorin extract, and the third peak corresponded to ginkgolide B. Figure 2B demonstrated that there were no remarkable differences in the effective permeability coefficients of paeoniflorin extract among the duodenum, jejunum, ileum and colon at concentrations of 5, 10 and 20 μg/mL. This suggests that the transport of paeoniflorin extract in the intestine occurs through passive diffusion.

Pharmacokinetics of paeoniflorin extract

Figure 3 illustrates HPLC profiles and the concentration-time curves of paeoniflorin extract in rat plasma samples after oral gavage with distinct concentrations of paeoniflorin extract. In Figure 3A, it was observed that, in contrast to the blank plasma sample (0 μg/mL), plasma samples after oral gavage with 5, 10 and 20 μg/mL of paeoniflorin extract experienced an additional characteristic peak corresponding to the chromatographic peak of paeoniflorin extract. This indicated that a higher concentration of paeoniflorin extract leads to a more prominent drug chromatographic peak. Figure 3B revealed that with the increase in paeoniflorin extract concentration, the changes in the concentration-time curve of paeoniflorin became more pronounced. The peak concentrations of paeoniflorin extract in plasma samples after oral gavage with 5, 10 and 20 μg/mL concentrations of paeoniflorin extract were reached around 4 hours, measuring 64.53, 148.35 and 318.03 μg/mL, respectively.

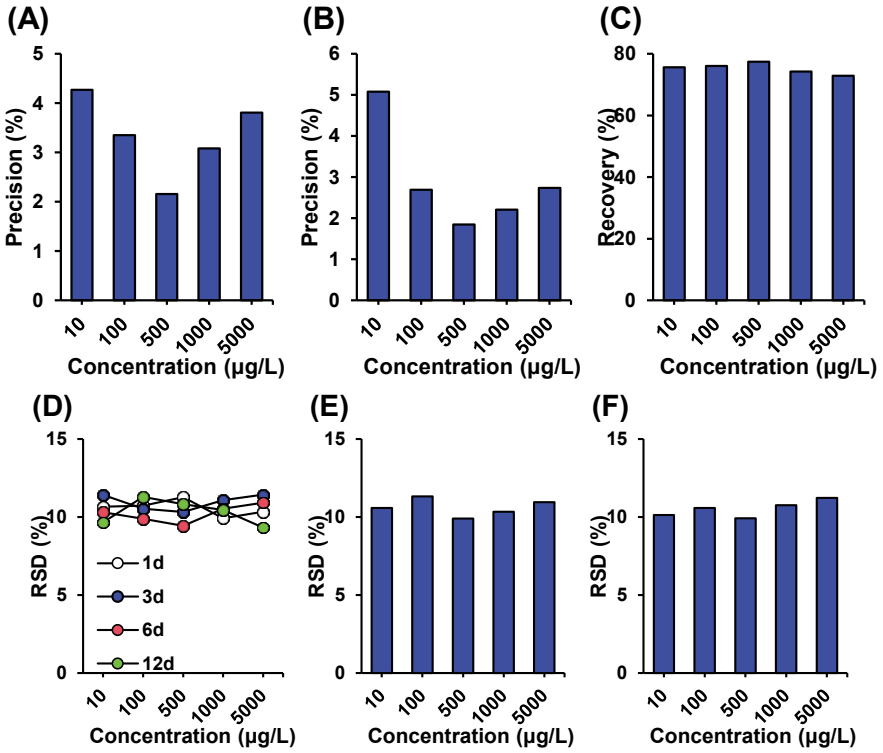

Figure 1.

Properties of paeoniflorin extract

(A) within-day precision; (B) inter-day precision; (C) recovery rate; (D) placement stability; (E) repeated freeze-thaw stability; and (F) cryopreservation stability.

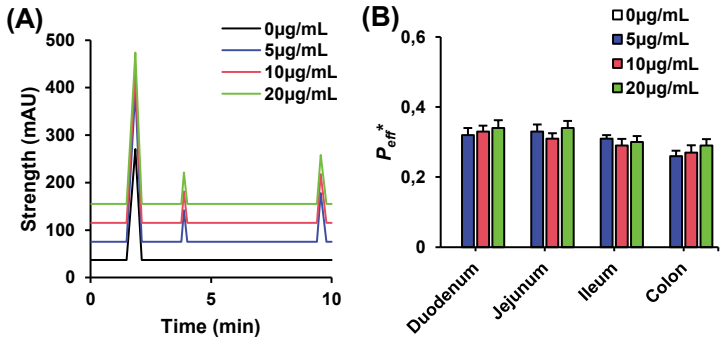

Figure 2.

Detection of intestinal perfusate samples

(A) HPLC profiles; (B): effective permeability coefficients.

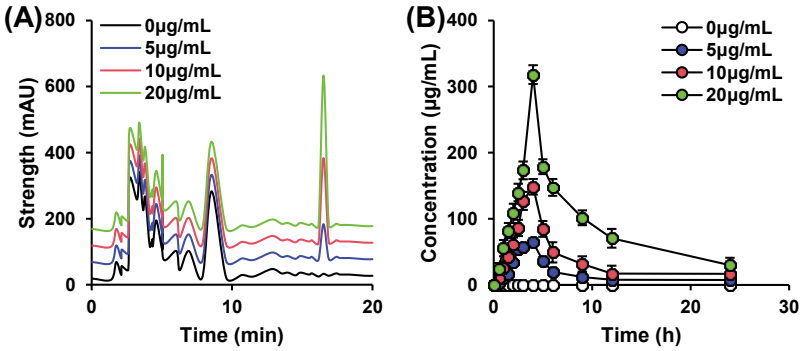

Figure 3.

Detection of plasma samples: (A) HPLC profiles; (B): concentration-time curves

Figure 4 depicts the differences in pharmacokinetic parameters after oral gavage with different concentrations of paeoniflorin extract. As the drug concentration increases, the absorption half-life (AHL) ranges from 0.667 to 1.124 hours (Figure 4A), the elimination half-life (EHL) ranges from 1.250 to 1.881 hours (Figure 4B), the peak concentration ranges from 64.532 to 318.031 μg/mL (Figure 4C), the peak time ranges from 3.512 to 3.790 hours (Figure 4D), and the area under the concentration-time curve (AUC) ranges from 281.962 to 1282.143 μg/h/L (Figure 4E). Overall, all parameters exhibit a gradual increasing trend.

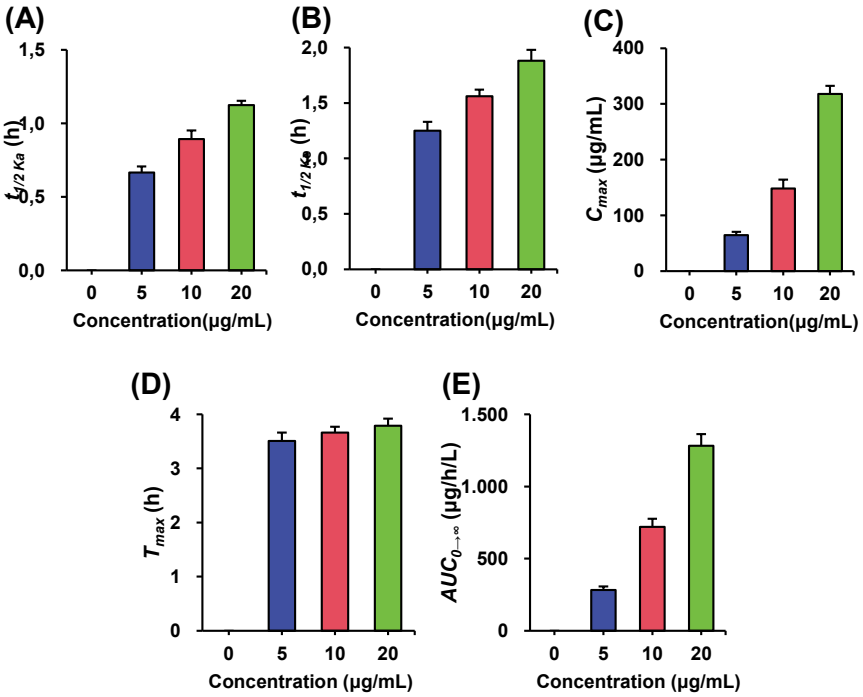

Figure 4.

Main pharmacokinetic parameters of paeoniflorin: (A): absorption half-life; (B): elimination half-life; (C): peak concentration; (D): time to reach peak concentration; (E): area under the concentration-time curve

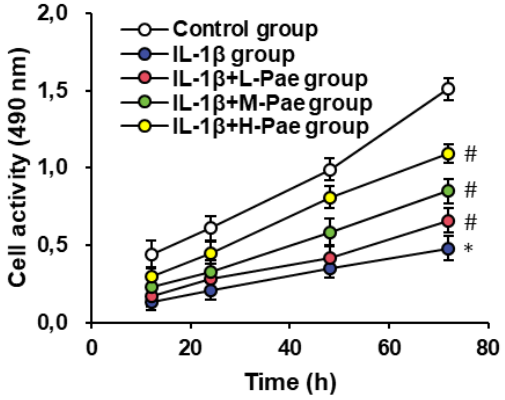

Figure 5.

Proliferation activity of chondrocytes of osteoarthritis

*p < 0.05 *vs*. Control group; #p < 0.05 *vs*. IL-1β group.

Impacts of paeoniflorin extract on proliferation and apoptosis of chondrocytes of osteoarthritis

Influences on the proliferation of chondrocytes of osteoarthritis. Figure 5 illustrates the impact of paeoniflorin extract on the proliferation of chondrocytes of osteoarthritis. It was evident that with the extension of culture time, the cell proliferation activity gradually increased in the Control group, IL-1β group, IL-1β+L-Pae group, IL-1β+M-Pae group and IL-1β+H-Pae group. Relative to the Control group, the cell proliferation activity in the IL-1β group was greatly decreased ($p < 0.05$). Meanwhile, the IL-1β+L-Pae group, IL-1β+M-Pae group and IL-1β+H-Pae group exhibited a remarkable increase in cell proliferation activity compared to the IL-1β group ($p < 0.05$), showing a concentration-dependent characteristic.

Impacts on apoptosis of chondrocytes of osteoarthritis. Figure 6 demonstrates the impact of paeoniflorin extract on the apoptosis of chondrocytes of osteoarthritis. In comparison to the Control group, the cell apoptosis rate in the IL-1β group was increased greatly, exhibiting an obvious difference ($p < 0.05$). IL-1β+L-Pae group, IL-1β+M-Pae group and IL-1β+H-Pae group experienced greatly decreased cell apoptosis rates based on the IL-1β group ($p < 0.05$), exhibiting a concentration-dependent characteristic.

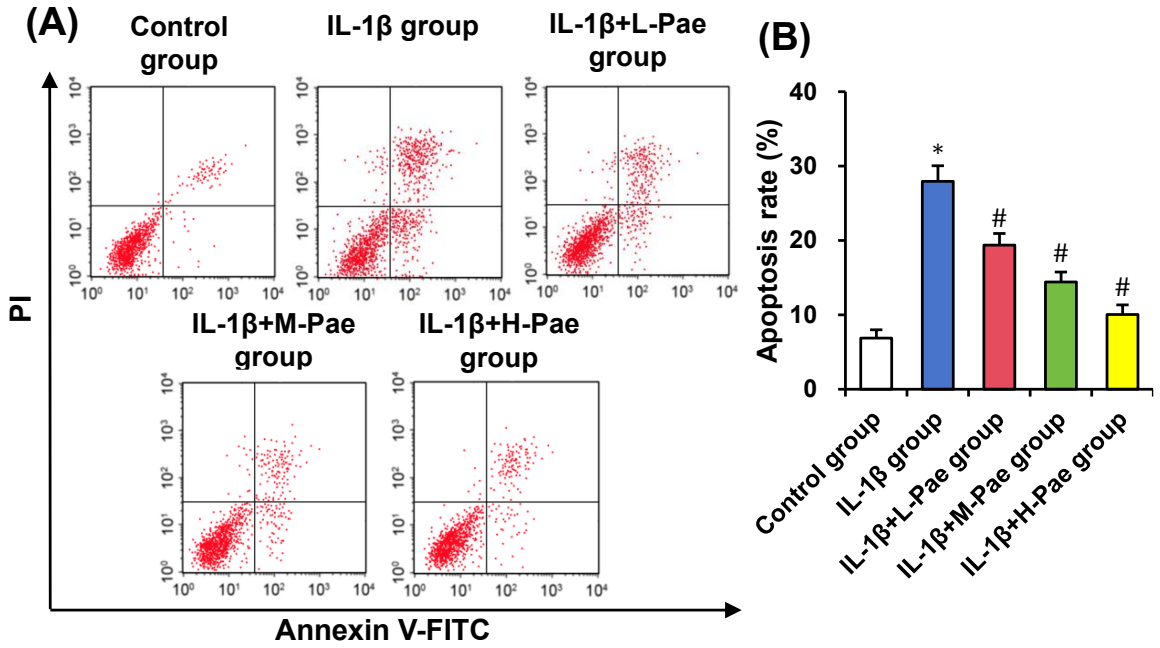

Figure 6.
Cell apoptosis for chondrocytes of osteoarthritis: (A) FCT-detected cell apoptosis; (B): cell apoptosis
*p < 0.05 *vs*. Control group; #p < 0.05 *vs*. IL-1β group.

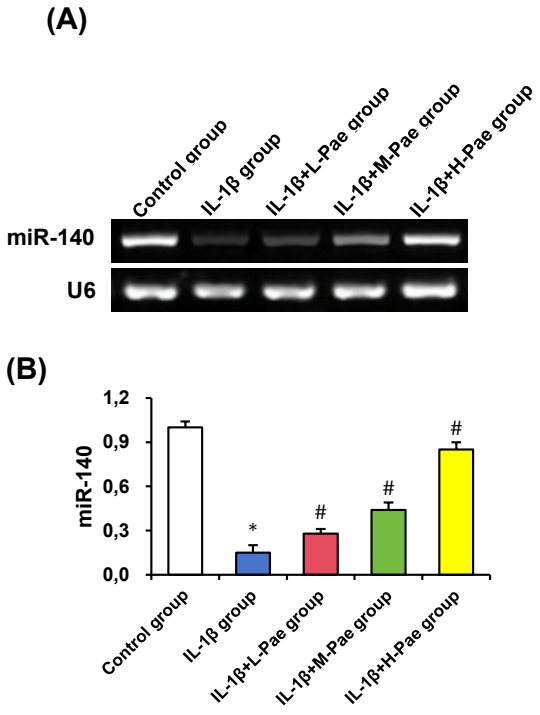

Figure 7.
miR-140 expression in chondrocytes of osteoarthritis: (A): PCR band; (B): miR-140 level
*p < 0.05 *vs*. Control group; #p < 0.05 *vs*. IL-1β group.

Impacts on miR-140 expression in chondrocytes of osteoarthritis. Figure 7 depicts the influence of the paeoniflorin extract on miR-140 expression in osteoarthritis chondrocytes. Relative to the Control group, the IL-1β group experienced a notable reduction in miR-140 expression, with a visible difference ($p < 0.05$). In comparison to the IL-1β group, the IL-1β+L-Pae group, IL-1β+M-Pae group and IL-1β+H-Pae group displayed a substantial elevation in cellular miR-140 level, presenting great differences ($p < 0.05$), indicating a concentration-dependent trend.

Impacts on the Wnt/β-catenin signalling pathway in chondrocytes of osteoarthritis. Figure 8 illustrates the impact of paeoniflorin extract on the levels of key proteins in the Wnt/β-catenin signalling pathway in chondrocytes of osteoarthritis. The figure signified that, relative to the Control group, the IL-1β group experiences a remarkable reduction in the DVL2, Cyclin D1 and β-catenin, while GSK-3β was elevated greatly ($p < 0.05$). When compared to the IL-1β group, the IL-1β+L-Pae group, IL-1β+M-Pae group and the IL-1β+H-Pae group showed a marked increase in DVL2, Cyclin D1 and β-catenin, coupled with a considerable decrease in GSK-3β expression ($p < 0.05$), indicating a concentration-dependent pattern.

Osteoarthritis is a degenerative chronic joint disease and a significant factor causing joint pain and disability in the elderly population. It predominantly occurs in weight-bearing joints such as the hip, knee and spine, with key pathological features including cartilage degeneration, disruptions in extracellular matrix synthesis and the formation of osteophytes that affect synovial tissue [16]. In TCM, osteoarthritis falls within the categories of "Bi (numb) Syndrome" and "Bone Bi Syndrome". The main etiological factors leading to this disease involve blood stasis, qi stagnation, wind-cold-dampness pathogens and deficiencies in nourishing tendons and bones. Treatment strategies often involve the use of tonifying the liver and kidney, promoting

blood circulation and resolving stasis-oriented medications for osteoarthritis [17-19]. paeoniflorin, a major active component in Chinese peony, has been investigated for its pharmacokinetic characteristics. It has been reported to promote T lymphocyte differentiation, exhibiting immunomodulatory effects [20]. Additionally, paeoniflorin can scavenge free radicals in the body, improving oxidative stress reactions [21]. This work examined the *in vivo* pharmacokinetic properties of paeoniflorin, revealing that it was absorbed to a certain extent in various intestinal segments. The uniform paeoniflorin effective permeability coefficients across different intestinal segments indicated its transport in the intestine occurs through passive diffusion. Furthermore, this work observed that at different concentrations, paeoniflorin exhibited an AHL of < 1.5 h, EHL of < 2.0 h, a peak concentration of > 50 μg/mL, a peak time of < 4 h, and an AUC of > 280 μg/h/L. This suggests that paeoniflorin is characterised by rapid absorption and efficient clearance in the body. Unabsorbed paeoniflorin undergoes metabolism by intestinal flora, generating three metabolites, which may contribute to reduced bioavailability [22]. Therefore, future research should explore strategies to enhance the bioavailability of paeoniflorin, which is crucial for improving therapeutic efficacy in disease management.

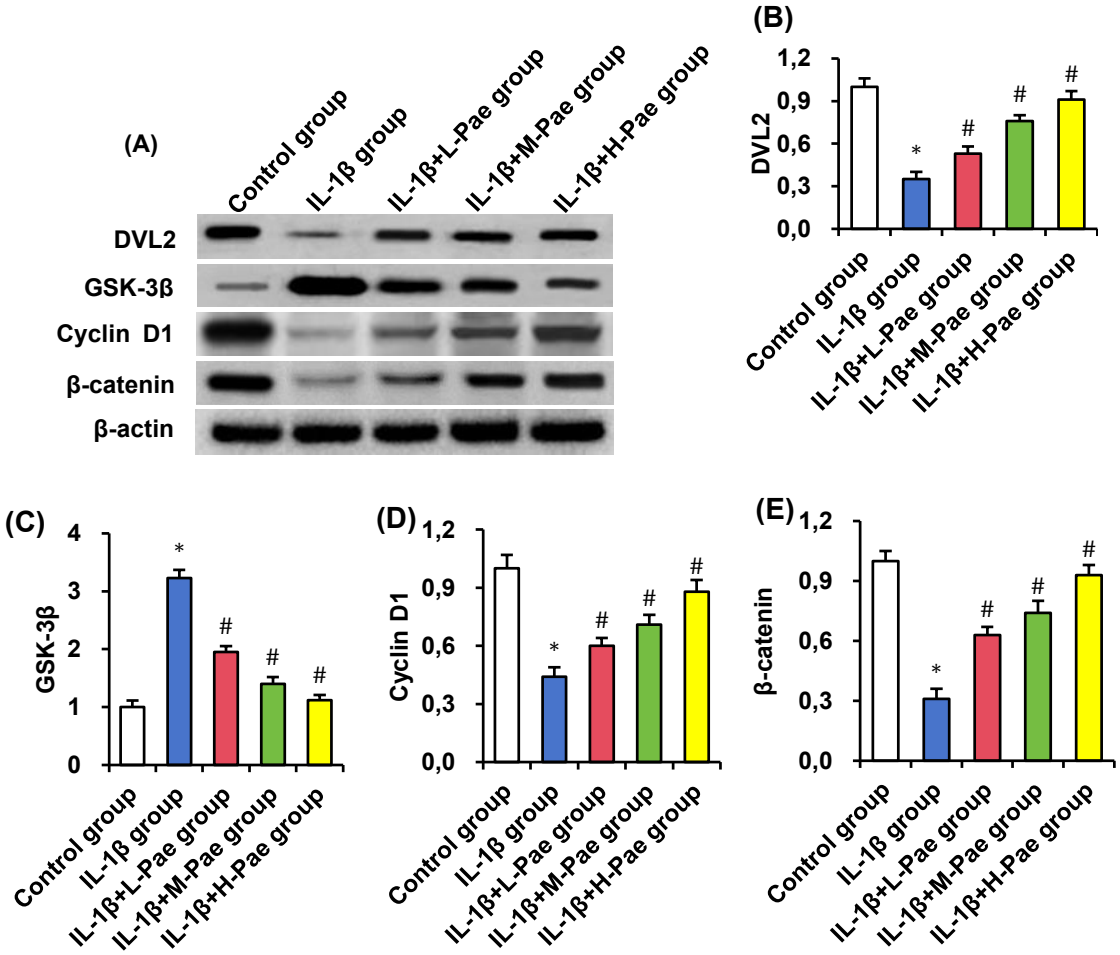

Figure 8.

Relevant proteins in Wnt/β-catenin signalling pathway of chondrocytes: (A) Western blot results; (B): DVL2; (C): GSK-3β; (D): Cyclin D1; (E): β-catenin.

*p < 0.05 *vs*. Control group; #p < 0.05 *vs*. IL-1β group.

Paeoniflorin can suppress the generation and release of inflammatory mediators, alleviating inflammatory reactions. Clinically, it is used for the treatment of diseases such as rheumatoid arthritis, systemic lupus erythematosus and other arthritis [23-25]. However, the mechanisms by which paeoniflorin affects the activities of chondrocytes in osteoarthritis, particularly cell proliferation and cell apoptosis, remain unclear. In the joint cells of osteoarthritis patients, inflammatory factors such as IL-1β are abnormally expressed, activating related signalling pathways, promoting imbalances in joint cell metabolism and exacerbating the severity of arthritis inflammation [26]. IL-1β serves as the initiating factor for inflammatory reactions and is highly expressed in the synovial fluid of osteoarthritis patients [27]. This work induced the normal human

chondrocytes with IL-1β to establish an *in vitro* osteoarthritis cell model. The results showed that IL-1β induction led to a decrease in chondrocyte cell proliferation activity and an increase in cell apoptosis, indicating that IL-1β induces chondrocyte apoptosis, consistent with the pathological features of abnormal apoptosis in osteoarthritis [28]. Subsequently, different concentrations of paeoniflorin were applied to IL-1β-induced chondrocytes, revealing that paeoniflorin significantly enhanced IL-1β-induced chondrocyte cell proliferation activity while inhibiting cell apoptosis. This is like the findings of Wu *et al*., who observed that paeoniflorin could reduce the proportion of IL-1β-induced apoptosis in rat cartilage [29]. These results suggest that paeoniflorin has potential therapeutic value as a treatment for osteoarthritis.

MiRNAs are extensively expressed in eukaryotic organisms and are involved in the regulation of chondrocyte cell proliferation and cell apoptosis. Duan *et al*. summarised that miR-140 plays a key role in promoting cartilage matrix remodelling, primarily by regulating the maturation of mesenchymal stem cell-derived cartilage [30]. Shi *et al*. [31] reported that in a mouse model with T-2 toxin-induced damage to joint cartilage and growth plates, the expression level of miR-140 decreased, suggesting its involvement in processes such as joint cartilage formation and extracellular matrix degradation. Chen, Huang *et al*. discovered that *in vitro* induction of rat chondrocytes with IL-1β led to a decrease in the expression level of miR-140-5p, and inhibiting miR-140-5p could exacerbate osteoarthritis-like changes [32]. This work revealed that after IL-1β induction in human chondrocytes, miR-140 expression decreased, indicating the involvement of miR-140 in the progression of osteoarthritis. Furthermore, this work found that paeoniflorin increased the miR-140 expression in chondrocytes induced by IL-1β. This suggests that paeoniflorin may regulate chondrocyte cell proliferation and cell apoptosis induced by IL-1β through the modulation of miR-140 expression. However, the precise mechanisms of action of miR-140 in osteoarthritis require further clarification.

The Wnt/β-catenin signalling pathway is involved in the regulation of various biological behaviours, including cell proliferation, differentiation, adhesion and polarity. Numerous studies have confirmed that abnormal activation of the Wnt/β-catenin signalling pathway, along with aberrant expression of Wnt and β-catenin proteins, exerts a crucial effect in activating downstream target molecules and regulating cell proliferation, invasion, apoptosis and the release of inflammatory factors [33-36]. Fan *et al*. demonstrated that inhibiting the activation of the Wnt/β-catenin signalling pathway stimulated by IL-1β could reverse the abnormal extracellular matrix metabolism in chondrocytes and exert a therapeutic effect in alleviating osteoarthritis of the ankle joint [37]. In the cytoplasm of cells, free β-catenin protein enters the cell nucleus, activating the transcription of downstream target genes such as Cyclin D1. Proteins like GSK-3β belong to the β-catenin protein degradation complex, regulating β-catenin levels in the cytoplasm. In the absence of Wnt ligands, GSK-3β promotes the phosphorylation of β-catenin, leading to its degradation and reduced expression levels [38]. DVL protein in the cytoplasm receives upstream signals, inhibiting the function of protein complexes such as GSK-3β, stabilising the free β-catenin protein in the cytoplasm [39]. This work unveiled that after IL-1β induction in human chondrocytes, DVL2, Cyclin D1 and β-catenin decreased, while GSK-3β increased. This indicates that IL-1β induction inhibits DVL2 in chondrocytes, promotes the formation of the GSK-3β complex, exacerbates the phosphorylation of β-catenin protein, and inhibits the transcription of downstream target genes like Cyclin D1, suggesting abnormal activation of the Wnt/β-catenin signalling pathway in osteoarthritis. Furthermore, this work signified that paeoniflorin treatment of IL-1β-induced chondrocytes resulted in increased DVL2, Cyclin D1 and β-catenin, and decreased GSK-3β. This indicates that paeoniflorin can inhibit the abnormal activation of the Wnt/β-catenin signalling pathway induced by IL-1β in chondrocytes, thereby promoting cell proliferation and inhibiting apoptosis.

Conclusions

Paeoniflorin extract can be absorbed in the intestine, and the drug concentration to some extent affects its pharmacokinetics in the body. Additionally, paeoniflorin extract could promote the proliferation of IL-1β-induced human chondrocytes while inhibiting apoptosis. This effect may be mediated by increased expression of miR-140 and the suppression of abnormal activation of the Wnt/β-catenin signalling pathway. These findings suggested that paeoniflorin extract held promise as a therapeutic agent for osteoarthritis.

Conflict of interest

The authors declare no conflict of interest.

References

1. Abramoff B, Caldera FE, Osteoarthritis: Pathology, Diagnosis, and Treatment Options. *Med Clin North Am*., 2020; 104(2): 293-311.
2. Molnar V, Matišić V, Kodvanj I, Bjelica R, Jeleč Ž, Hudetz D, Rod E, Čukelj F, Vrdoljak T, Vidović D, Starešinić M, Sabalić S, Dobričić B, Petrović T, Antičević D, Borić I, Košir R, Zmrzljak UP, Primorac D, Cytokines and chemokines involved in osteoarthritis pathogenesis. *Int J Mol Sci*., 2021; 22(17): 9208.
3. van den Bosch MHJ, Osteoarthritis year in review 2020: biology. *Osteoarthritis Cartilage*, 2021; 29(2): 143-150.
4. Roseti L, Desando G, Cavallo C, Petretta M, Grigolo B, Articular Cartilage Regeneration in Osteoarthritis. *Cells,* 2019; 8(11): 1305.

5. Stefanovici Zugravu G, Dimitriu DC, Ciobanu CP, Tamba BI, Ciorpac M, Mihai CT, Cumpat CM, Brebu M, Mandici A, Panainte AD, Trifan A, Miron A, Benefits of *Sea buckthorn* fruit oil as adjuvant therapy in rheumatoid arthritis. *Farmacia*, 2024; 72(3): 554-564.
6. Lv S, Zhao Y, Wang L, Yu Y, Li J, Huang Y, Xu W, Sun G, Dai W, Zhao T, Bi D, Ma Y, Sun P, Anti-depressant active components of *Bupleurum chinense* DC - *Paeonia lactiflora* Pall Herb Pair: Pharmacological mechanisms. *Biomed Res Int.,* 2022; 2022: 1024693.
7. Yan BF, Chen X, Chen YF, Liu SJ, Xu CX, Chen L, Wang WB, Wen TT, Zheng X, Liu J, Aqueous extract of *Paeoniae Radix Alba* (*Paeonia lactiflora* Pall.) ameliorates DSS-induced colitis in mice by tunning the intestinal physical barrier, immune responses, and microbiota. *J Ethnopharmacol*., 2022; 294: 115365.
8. Wang XL, Feng ST, Wang YT, Chen NH, Wang ZZ, Zhang Y, Paeoniflorin: A neuroprotective monoterpenoid glycoside with promising anti-depressive properties. *Phytomedicine*, 2021; 90: 153669.
9. Wang Y, Zhou Y, Lin H, Chen H, Wang S, Paeoniflorin Inhibits the Proliferation and Metastasis of Ulcerative Colitis-Associated Colon Cancer by Targeting EGFL7. *J Oncol*., 2022; 2022: 7498771.
10. Chen Y, Zhang G, Cao D, Wang F, Zhang F, Shao H, Jiao W, New Monoterpene Glycoside Paeoniflorin Derivatives as NO and IL-1β Inhibitors: Synthesis and Biological Evaluation. *Molecule,* 2023; 28(19): 6922.
11. Xu L, Wang H, Yu QQ, Ge JR, Zhang XZ, Mei D, Liang FQ, Cai XY, Zhu Y, Shu JL, Tai Y, Wei W, Zhang LL, The monomer derivative of paeoniflorin inhibits macrophage pyroptosis *via* regulating TLR4/ NLRP3/ GSDMD signalling pathway in adjuvant arthritis rats. *Int Immunopharmacol*., 2021; 101(Pt A): 108169.
12. Vértiz-Hernández AA, Ponce-Peña P, Teránfigueroa Y, De Jesús Pozos-Guillén A, Rodríguez RA, Hernández JAV, De Jesús Rangel-López A, Montero-Morán GM, Local antinociceptive effect of "snow mountain garlic" in an experimental formalin model. *Farmacia*, 2023; 71(1): 11-17.
13. Zhang Y, Yang X, Han C, Wang D, Ma Y, Wei W, Paeoniflorin-6'O-benzene sulfonate suppresses fibro-blast-like synoviocytes proliferation and migration in rheumatoid arthritis through regulating GRK2-Gβγ interaction. *Exp Ther Med*., 2022; 24(2): 523.
14. Alharbi KS, Afzal O, Altamimi ASA, Almalki WH, Kazmi I, Al-Abbasi FA, Alzarea SI, Makeen HA, Albratty M, Potential role of nutraceuticals *via* targeting a Wnt/β-catenin and NF-κB pathway in treatment of osteoarthritis. *J Food Biochem*., 2022; 46(12): e14427.
15. Rajagopal K, Arjunan P, Marepally S, Madhuri V, Controlled Differentiation of Mesenchymal Stem Cells into Hyaline Cartilage in miR-140-Activated Collagen Hydrogel. *Cartilage*, 2021;13(2): 571S-581S.
16. Motta F, Barone E, Sica A, Selmi C, Inflammaging and Osteoarthritis. *Clin Rev Allergy Immunol.,* 2023; 64(2): 222-238.
17. Wen-Yue W, Ying-Peng X, Quan-Mao D, Li-Min X, De-Zhi W, Yang B, Li-Su W, Yu-Bin L, Zhi-Jun N, Yan-Xu M, Wu-Zhong C, Li-Qun B, Yang L, Li-Kun J, A randomised, parallel control and multicentre clinical trial of evidence-based traditional Chinese medicine massage treatment *vs.* External Diclofenac Diethylamine Emulgel for the treatment of knee osteoarthritis. *Trials*, 2022; 23(1): 555.
18. Li R, Chen H, Feng J, Xiao Y, Zhang H, Lam CW, Xiao H, Effectiveness of Traditional Chinese Exercise for Symptoms of Knee Osteoarthritis: A Systematic Review and Meta-Analysis of Randomised Controlled Trials. *Int J Environ Res Public Health*, 2020; 17(21): 7873.
19. Sun Q, Zhang K, Chen J, Xu Y, Liu Y, Zheng R, Traditional Chinese medicine classification of knee osteoarthritis with proteomics analysis. *Ann Palliat Med*., 2020; 9(6): 3750-3756.
20. Ji L, Wang S, Wu S, Bao J, Xie G, Zhang Y, Xu L, Lin N, Wang J, Fan Y, Fu D, Dai Q, Paeoniflorin Inhibits LPS-Induced Activation of Splenic CD4+ T Lymphocytes and Relieves Pathological Symptoms in MRL/lpr Mice by Suppressing IRAK1 Signalling. *Evid Based Complement Alternat Med*., 2022; 2022: 5161890.
21. Peng W, Chen Y, Tumilty S, Liu L, Luo L, Yin H, Xie Y, Paeoniflorin is a promising natural monomer for neurodegenerative diseases *via* modulation of Ca^{2+} and ROS homeostasis. *Curr Opin Pharmacol*., 2022; 62: 97-102.
22. Wang Y, You K, You Y, Li Q, Feng G, Ni J, Cao X, Zhang X, Wang Y, Bao W, Wang X, Chen T, Li H, Huang Y, Lyu J, Yu S, Li H, Xu S, Zeng K, Shen X, Paeoniflorin prevents aberrant proliferation and differentiation of intestinal stem cells by controlling C1q release from macrophages in chronic colitis. *Pharmacol Res*., 2022; 182: 106309.
23. Qu B, Wang XL, Zheng DC, Mai CT, Liu ZQ, Zhou H, Xie Y, Novel treatment for refractory rheumatoid arthritis with total glucosides of paeony and nobiletin codelivered in a self-nanoemulsifying drug delivery system. *Acta Pharmacol Sin*., 2022; 43(8): 2094-2108.
24. Ma J, Meng Q, Zhan J, Wang H, Fan W, Wang Y, Zhang S, Bian H, Zheng F, Paeoniflorin Suppresses Rheumatoid Arthritis Development *via* Modulating the Circ-FAM120A/miR-671-5p/MDM4 Axis. *Inflammation*, 2021; 44(6): 2309-2322.
25. Zhang XX, Zuo JQ, Wang YT, Duan HY, Yuan JH, Hu YH, Paeoniflorin in *Paeoniaceae*: Distribution, influencing factors, and biosynthesis. *Front Plant Sci*., 2022; 13: 980854.
26. Chien SY, Tsai CH, Liu SC, Huang CC, Lin TH, Yang YZ, Tang CH, Noggin Inhibits IL-1β and BMP-2 Expression and Attenuates Cartilage Degeneration and Subchondral Bone Destruction in Experimental Osteoarthritis. *Cells*, 2020; 9(4): 927.
27. Hwang HS, Lee MH, Go DJ, Kim HA, Norepinephrine modulates IL-1β-induced catabolic response of human chondrocytes. *BMC Musculoskelet Disord*., 2021; 22(1): 724.
28. Liao CR, Wang SN, Zhu SY, Wang YQ, Li ZZ, Liu ZY, Jiang WS, Chen JT, Wu Q, Advanced oxidation protein products increase TNF-α and IL-1β expression in chondrocytes *via* NADPH oxidase 4 and accelerate cartilage degeneration in osteoarthritis progression. *Redox Biol*., 2020; 28: 101306.
29. Wu L, Tang R, Xiong W, Song S, Guo Q, Zhang Q, Paeoniflorin shows chondroprotective effects under

IL-1β stress by regulating circ-PREX1/miR-140-3p/WNT5B axis. *J Orthop Surg Res*., 2023; 18(1): 766.
30. Duan L, Liang Y, Xu X, Xiao Y, Wang D, Recent progress on the role of miR-140 in cartilage matrix remodelling and its implications for osteoarthritis treatment. *Arthritis Res Ther*., 2020; 22(1): 194.
31. Shi Y, Shao X, Sun M, Ma J, Li B, Zou N, Li F, MiR-140 is involved in T-2 toxin-induced matrix degradation of articular cartilage. *Toxicon*., 2023; 222: 106987.
32. Chen Y, Huang H, Zhong W, Li L, Lu Y, Si HB, miR-140-5p protects cartilage progenitor/stem cells from fate changes in knee osteoarthritis. *Int Immunopharmacol*., 2023; 114: 109576.
33. Mahajan A, Nengroo MA, Datta D, Katti DS, Converse modulation of Wnt/β-catenin signalling during expansion and differentiation phases of *Infrapatellar* fat pad-derived MSCs for improved engineering of hyaline cartilage. *Biomaterials,* 2023; 302: 122296.
34. Colozza G, Koo BK, Wnt/β-catenin signalling: Structure, assembly and endocytosis of the signalosome. *Dev Growth Differ*., 2021; 63(3): 199-218.
35. Brănescu C, Serban D, Dascălu AM, Oprescu SM, Savlovschi C, Interleukin 6 and lipopolysaccharide binding protein - markers of inflammation in acute appendicitis. *Chirurgia (Bucharest)*, 2013; 108(2): 206-214.
36. Silva-García O, Valdez-Alarcón JJ, Baizabal-Aguirre VM, Wnt/β-Catenin Signalling as a Molecular Target by Pathogenic Bacteria. *Front Immunol*., 2019; 10: 2135.
37. Fan Z, Zhao X, Ma J, Zhan H, Ma X, Suppression of YAP Ameliorates Cartilage Degeneration in Ankle Osteoarthritis *via* Modulation of the Wnt/β-Catenin Signalling Pathway. *Calcif Tissue Int*., 2024; 115(3): 283-297.
38. Vallée A, Lecarpentier Y, Vallée JN, Cannabidiol and the Canonical WNT/β-Catenin Pathway in Glaucoma. *Int J Mol Sci*., 2021; 22(7): 3798.
39. Zhu Y, Li Y, Jin W, Li Z, Zhang L, Fang Y, Zhang Y, Hyperoxia exposure upregulates Dvl-1 and activates Wnt/β-catenin signalling pathway in newborn rat lung. *BMC Mol Cell Biol*., 2023; 24(1): 4.